Metabolic Engineering Communications 10 (2020) e00124

Contents lists available at ScienceDirect

Metabolic Engineering Communications

journal homepage: www.elsevier.com/locate/mec

Metabolic engineering of an acid-tolerant yeast strain *Pichia kudriavzevii* for itaconic acid production

Wan Sun [a], Ana Vila-Santa [b], Na Liu [c], Tanya Prozorov [d], Dongming Xie [c], Nuno Torres Faria [b], Frederico Castelo Ferreira [b], Nuno Pereira Mira [b,**], Zengyi Shao [a,d,e,f,*]

[a] *Interdepartmental Microbiology Program, Iowa State University, Ames, USA*
[b] *Department of Bioengineering, Instituto Superior Técnico, Lisbon, Portugal*
[c] *Department of Chemical Engineering, University of Massachusetts, Lowell, MA, USA*
[d] *Ames Laboratory, U.S. Department of Energy, Ames, Iowa, USA*
[e] *Department of Chemical and Biological Engineering, Iowa State University, Ames, USA*
[f] *NSF Engineering Research Center for Biorenewable Chemicals, Iowa State University, Ames, USA*

ARTICLE INFO

Keywords:
Pichia kudriavzevii
Issatchenkia orientalis
Non-conventional microorganisms
Itaconic acid
Biopolymers
Acid tolerance

ABSTRACT

Itaconic acid (IA), or 2-methylenesuccinic acid, has a broad spectrum of applications in the biopolymer industry owing to the presence of one vinyl bond and two acid groups in the structure. Its polymerization can follow a similar mechanism as acrylic acid but additional functionality can be incorporated into the extra beta acid group. Currently, the bio-based production of IA in industry relies on the fermentation of the filamentous fungus *Aspergillus terreus*. However, the difficulties associated with the fermentation undertaken by filamentous fungi together with the pathogenic potential of *A. terreus* pose a serious challenge for industrial-scale production. In recent years, there has been increasing interest in developing alternative production hosts for fermentation processes that are more homogenous in the production of organic acids.

Pichia kudriavzevii is a non-conventional yeast with high acid tolerance to organic acids at low pH, which is a highly desirable trait by easing downstream processing. We introduced *cis*-aconitic acid decarboxylase gene (*cad*) from *A. terreus* (designated *At_cad*) into this yeast and established the initial titer of IA at 135 ± 5 mg/L. Subsequent overexpression of a native mitochondrial tricarboxylate transporter (herein designated *Pk_mttA*) presumably delivered *cis*-aconitate efficiently to the cytosol and doubled the IA production. By introducing the newly invented CRISPR-Cas9 system into *P. kudriavzevii*, we successfully knocked out both copies of the gene encoding isocitrate dehydrogenase (*ICD*), aiming to increase the availability of *cis*-aconitate. The resulting *P. kudriavzevii* strain, devoid of *ICD* and overexpressing *Pk_mttA* and *At_cad* on its genome produced IA at 505 ± 17.7 mg/L in shake flasks, and 1232 ± 64 mg/L in fed-batch fermentation. Because the usage of an acid-tolerant species does not require pH adjustment during fermentation, this work demonstrates the great potential of engineering *P. kudriavzevii* as an industrial chassis for the production of organic acid.

1. Introduction

Due to growing concerns regarding the unsustainability of producing chemicals from petroleum and the associated environmental impacts, researchers have been working on identifying alternative microbial platforms for the conversion of biomass-derived feedstock into various commodity and specialty chemicals (Choi et al., 2015; Curran and Alper, 2012). Itaconic acid (IA) is an unsaturated C5 dicarboxylic acid with a methylene group connected to the C2 group of succinic acid (hence also known as 2-methylenesuccinic acid). It was selected as a top building block chemical in the report of the Department of Energy (DOE) in 2004 (Werpy and Petersen, 2004) and its market is estimated to reach 52,000 tons/year and 260 million dollars in 2025 (De Carvalho, Magalhaes, and Soccol, 2018). IA can be used as a specialty co-monomer in the synthesis of resins, fibers, adhesives, thickeners, and binders (El-Imam and Du, 2014). For example, the co-polymer poly-(acrylamide-co-itaconic acid) has a super-absorbent ability and therefore can be used in diapers and hygiene products (El-Imam and Du, 2014). The tri-functional structure (one methylene

* Corresponding author. 4140 Biorenewables Research Laboratory, Iowa State University, Ames, IA, 50011, USA.
** Corresponding author. Department of Bioengineering, Instituto Superior Técnico Avenida Rovisco Pais, Lisbon, 1049-001, Portugal.
E-mail addresses: nuno.mira@ist.utl.pt (N.P. Mira), zyshao@iastate.edu (Z. Shao).

https://doi.org/10.1016/j.mec.2020.e00124
Received 2 October 2019; Received in revised form 6 January 2020; Accepted 27 January 2020

group and two carboxyl groups) of IA allows it to take similar conversions as maleic acid and be readily derivatized to a wide spectrum of valuable chemicals (e.g., itaconic diamide, 2-methyl-1,4-butanediamine, 2-methyl-1,4-butanediol, 3-methyl tetrahydrofuran, and 3-methyl-gamma-butyrolactone) (Saha, 2017). Considering that it shares its basic structure with acrylic acid (containing both alpha acid and vinyl bond), on top of which it incorporates an additional beta acid group that can bring additional desired functionalities, IA has a great potential to supplement the $20 billion market established for acrylic acid.

Unlike the nonrenewable process for acrylic acid production, IA can be easily converted in one decarboxylation step from *cis*-aconitate, an intermediate of the tri-carboxylic acid (TCA) cycle. The current production of IA at an industrial scale is enabled by fermenting the filamentous fungus *A. terreus*, with a titer of 160 g/L (Krull et al., 2017) that is close to the theoretical number. However, industrial-scale production *via* fermentation undertaken by filamentous fungi is constrained by great difficulties in reproducibility of the fermentation and, consequently, costly production processes. The highly branched mycelial filaments give rise to a high broth viscosity during fermentation, which results in significant challenges in both the mixing and aeration processes in conventional agitated tank fermenters (Porro and Branduardi, 2017). The continuously altered rheological properties of the broth pose stringent requirements for process design, and the production capacities and efficiencies will otherwise dramatically decrease in large-scale aerobic fermentation processes. Also, *A. terreus* is considered a biosafety level 2 organism in multiple European countries and the US due to its potential to produce toxins (De Hoog, 1996).

All these reasons have motivated researchers to search for alternative hosts, ranging from the natural producers *Ustilago maydis* (Geiser et al., 2016) and *Ustilago cynodontis* (Tehrani et al., 2019), to the heterologous hosts including *Aspergillus niger* (van der Straat et al., 2014; Hossain et al., 2016; (Blumhoff et al., 2013), *Saccharomyces cerevisiae* (Blazeck et al., 2014; Young et al., 2018), *Yarrowia* lipolytica (Blazeck et al., 2015; Zhao et al., 2019), *Escherichia coli* (Harder et al., 2016; Tran et al., 2019; Vuoristo et al., 2015), and *Corynebacterium glutamicum* (Otten et al., 2015). Despite the improvements, to date, none of these hosts have been reported to generate IA at a level comparable to that attained by *A. terreus*.

Another important aspect that is often ignored in lab-scale fermentation but plays an essential role in the design of large-scale industrial processes for organic acid production is, whether neutralization is required during production. For many microbial hosts, the limited growth at an acidic pH coupled with the toxicity exerted by the accumulation of the organic acid in the preferred undissociated form pose a need to adjust the pH of the broth with an alkaline (e.g., $Ca(OH)_2$) to ensure that the growth of the host is not hindered. Consequently, a subsequent step typically conducted with a strong acid (e.g., H_2SO_4) is required to recover the organic acid in its undissociated form. This practice implies significant costs on the acid and base, in addition to the production of an enormous amount of gypsum (i.e., $CaSO_4$) that is ultimately released into the environment. The use of acid-tolerant microbial species is a promising way to address this issue, especially now that the ability to genetically manipulate non-model microorganisms has seen dramatic improvement in recent years.

Pichia kudriavzevii (also known as *Issatchenkia orientalis*) is a non-conventional yeast that exhibits multi-stress tolerance towards low pH, high temperature, and high salt concentration. The potential of engineering *P. kudriavzevii* for the synthesis of organic acids has been demonstrated in the production of xylonic acid, lactic acid, and succinic acid (Park et al., 2018; Toivari et al., 2013; Xiao et al., 2014). These traits, together with the availability of a draft genomic sequence, have rendered interest in engineering *P. kudriavzevii* as a potential producer of IA under acidic conditions. To mitigate plasmid instability, we developed a CRISPR-Cas9-mediated genome-editing strategy and integrated *At_cad* and the native *Pk_mttA* genes into the genome of a mutant carrying the isocitrate dehydrogenase gene (*ICD*) knockout. The final strain produced IA at 1232 ± 64 mg/L with a yield of 29 ± 1.2 mg IA/g glucose and a productivity of 51 mg/L/h in a fed-batch fermenter. In light of the need for significant endeavors to reach an IA production level of commercial interest, our work presents the strategies to engineer the IA biosynthetic pathway in an acid-tolerant species, expanding the current collection of microbial factories suitable for fermentation at low pH.

2. Materials and methods

2.1. Strains, media, and materials

P. kudriavzevii NRRL Y134, Y870, Y27916, YB236, and YB4010 were requested from the ARS Culture Collection. *S. cerevisiae* CEN.PK113-7D and INVSc1 are two common laboratory strains. *S. cerevisiae* YSG50 (*MATα*, *ade2-1*, *ade3Δ22*, *ura3-1*, *his3-11,15*, *trp1-1*, *leu2-3,112*, and *can1-100*) was used as the host for plasmid assembly using the DNA assembler procedure (Shao et al., 2012; Shao and Zhao, 2014). *E. coli* strain BW25141 was used for plasmid propagation.

YPD medium containing 1% yeast extract, 2% peptone, and 2% dextrose was used to grow *P. kudriavzevii*; YPAD medium containing 1% yeast extract, 2% peptone, 2% dextrose, and 0.01% adenine hemisulfate was used to grow *S. cerevisiae* YSG50. Synthetic complete dropout medium lacking uracil (SC-URA) containing 0.5% ammonium sulfate, 0.16% yeast nitrogen without amino acid and ammonium sulfate, CSM-URA (added according to manufacturer's instruction), 0.043% adenine hemisulfate, and 2% dextrose, was used to select the yeast transformants containing the assembled plasmids. Antifoam 204 was purchased from Sigma (St. Louis, MO).

The Wizard Genomic DNA Purification Kit was purchased from Promega (Madison, WI). Q5 High-Fidelity DNA Polymerase was purchased from New England Biolabs (Ipswich, MA). FastDigest restriction enzymes were purchased from Thermo Fisher Scientific (Waltham, MA). The QIAprep Spin Plasmid Mini-prep Kit and RNeasy Mini Kit were purchased from Qiagen (Valencia, CA). Zymolyase, Zymoprep Yeast Plasmid Miniprep II Kit, and Zymoclean Gel DNA Recovery Kit were purchased from Zymo Research (Irvine, CA). RevertAid First Strand cDNA Synthesis Kit was purchased from Thermo Scientific (Waltham, MA). Yeast nitrogen base without amino acids and ammonium sulfate, yeast extract, peptone, agar, and other reagents required for cell culture were obtained from Difco (Franklin Lakes, NJ). Luria Bertani (LB) broth, ammonium sulfate, glucose, and other chemicals were obtained from Thermo Fisher Scientific (Waltham, MA). Amino acid mixture lacking uracil (CSM-URA) was purchased from MP Biomedicals (Santa Ana, CA). Oligonucleotides and gBlocks were obtained from Integrated DNA Technologies (Coralville, IA).

2.2. Plasmid construction

The plasmids and strains used in this study are listed in Supplementary Materials Tables S1 and S2. Important gene sequences from *P. kudriavzevii* are listed in Table S3. To construct the episomal plasmid for *P. kudriavzevii*, pRS416 was digested by *XbaI*/*Xho*I and used as the plasmid assembly backbone. The previously identified 91-bp autonomously replicating sequence (ARS) (Xiao et al., 2014), the *URA3* expression cassette amplified from *P. kudriavzevii* genome, and the gene encoding green fluorescence protein (GFP) were designed to have homologous arms with the neighboring fragments, and co-transformed into *S. cerevisiae* YSG50 *via* the DNA assembler procedure (Shao et al. 2012; Shao and Zhao 2014)to yield the plasmid pWS-Pk-URA-GFP (Fig. S1). This plasmid was verified by restriction digestion and sequencing, and then used as the backbone for constructing other plasmids in this study.

To construct the plasmids for IA production, the gene encoding *cis*-aconitate decarboxylase (*cad*) from *A. terreus* was synthesized with optimized codons. The mitochondrial tricarboxylate transporter (*Pk_mttA*, C5L36_0C10570)was amplified from the *P. kudriavzevii* genome. It was cloned into the backbone of the plasmid pWS-Pk-URA-

GFP, replacing GFP *via* homologous recombination.

To develop CRISPR-Cas9-based genetic manipulation tools, five different versions of Cas9 (described below in the Results section) were amplified from the reported plasmids (Bao et al., 2015; Cao et al., 2018; DiCarlo et al., 2013; Vyas et al., 2015; Cong et al., 2013). These Cas9 genes were flanked by SV40 nuclear localization signals at both ends and a FLAG tag at the front of SV40 at the 5' end. The synthetic guide RNA (gRNA) cassette for gene deletion contained a 20-bp guide sequence designed using the CHOPCHOP web tool (Montague et al., 2014). All of the fragments, together with the plasmid backbone, were assembled using the DNA assembler method (Shao et al. 2012; Shao and Zhao 2014) *via* homologous recombination. All of the plasmids were confirmed by sequencing at the Iowa State University DNA Facility.

2.3. IA tolerance assay

To select an IA-tolerant *P. kudriavzevii* strain, five *P. kudriavzevii* strains, NRRL Y134, Y870, Y27916, YB236, and YB4010, together with two commonly used *S. cerevisiae* strains, CEN.PK113-7D (haploid) and INVSc1 (diploid), were evaluated. All seven strains were cultured overnight in 3-mL SC medium (pH 5.6) in 15-mL culture tubes as seed cultures, which were then inoculated to an initial OD_{600} of 0.2 in 3-mL SC medium containing different concentrations of IA, ranging from 0 to 50 g/L, either with pH adjusted to 5.6 (using 10 M NaOH) or without pH adjustment. The cell densities were measured after cultivation at 30 °C with 250 rpm orbital shaking after 10 h. The assay was performed in three biological replicates.

2.4. Strain construction

For GFP expression and IA production in *P. kudriavzevii*, the corresponding plasmids were transformed into *P. kudriavzevii* YB4010 *ura3Δ* by electroporation using a voltage of 1.5 kV. The transformants were selected on agar plates containing synthetic complete medium lacking uracil (SC-URA).

To evaluate the performance of the CRISPR-Cas9 system, the *ADE2* locus was selected as the first target. Briefly, 1 μg of plasmid (e.g., pWS-iCas9-RPR1-ADE2) was transformed into *P. kudriavzevii* YB4010 *ura3Δ* by electroporation, immediately followed by cell recovery in 1-mL liquid YPAD medium for 3 h. The cells were subsequently centrifuged, washed three times with 1 M sorbitol, and plated on the SC-URA plates supplemented with 55 mg/mL of adenine hemisulfate. The plates were incubated at 30 °C until colonies appeared (about 3 days). The colonies were re-streaked on fresh SC-URA plates containing 10 mg/mL of adenine hemisulfate. Pink colonies were inoculated into SC-URA liquid medium and grown for 2 days. Genomic DNA was extracted using the Wizard Genomic DNA Purification Kit and then used as a template for diagnostic PCR. The PCR product was recovered from agarose gel and sequenced to confirm the mutation.

To construct the *icd* knockout strain, 1 μg of plasmid pWS-iCas9-RPR1-ICD and 1 μg of donor DNA, were co-transformed into *P. kudriavzevii* YB4010 *ura3Δ* and plated on the SC-URA plates. The donor DNA consisted of 500 bp homologous arms that were amplified from both the upstream and downstream regions of *ICD* and then fused by overlap extension PCR. To integrate the IA pathway into the *P. kudriavzevii* genome, a donor DNA containing the expression cassettes of *At_cad* and *Pk_mttA*, flanked by 500 bp homologous arms to the upstream and downstream regions of *ADE2*, was co-transformed with the plasmid pWS-iCas9-RPR1-ADE2 into both *P. kudriavzevii* YB4010 *ura3Δ* and the *ura3ΔicdΔ* strains. The transformants were plated on SC-URA plates for selection. The resulting strains were confirmed by diagnostic PCR and sequencing.

2.5. Flow cytometry analysis

A single colony of the *P. kudriavzevii* strain bearing the pWS-Pk-URA-GFP plasmid was cultured in 3-mL SC-URA medium for approximately 24 h. The *S. cerevisiae* strain containing pRS416-GFP was used as a reference. Briefly, 10 μL of the cell culture was diluted in 10 mM phosphate-buffered saline (pH 7.4) to an OD_{600} of 0.1. The samples were analyzed by flow cytometry at 488 nm with a FACSCanto flow cytometer (BD Biosciences, San Jose, CA). BD FACSCanto Clinical Software was used to evaluate the flow cytometry data.

2.6. Quantitative PCR

The strength of guide RNA promoter was evaluated by quantitative PCR (qPCR). Single colonies were picked from SC-URA plates after transforming the CRISPR-Cas9 plasmid designed to target the *ADE2* locus using RPR1p as the promoter for gRNA. The colonies were cultured in 3-mL SC-URA medium for 24 h. The total RNA was isolated using QIAGEN RNeasy Mini Kit and converted to cDNA *via* reverse transcription using RevertAid First Strand cDNA Synthesis Kit according to the manufacturers' instructions. qPCR was performed on a StepOnePlus Real-Time PCR system (Thermo Scientific, Waltham, MA) using SYBR green as a reporter. The actin gene *ACN1* was used as an internal control. The experiments were performed with three biological replicates.

2.7. Fermentation

For batch fermentation, single colonies of *P. kudriavzevii* strains with different genetic manipulations (Table S2) were inoculated into 3-mL SC-URA liquid medium and cultured for approximately 1.5 days. Cells were collected by centrifugation, washed twice with water, transferred into 10-mL of SC-URA liquid medium with an initial OD_{600} of 0.2, and cultivated at 30 °C with 250 rpm orbital shaking in 50-mL glass tubes. Samples were collected every 24 h for 7 days for HPLC analysis. The experiments were conducted with three biological replicates.

For fed-batch fermentation, the seed culture was prepared by inoculating a single colony of the *P. kudriavzevii ura3Δicd1Δade2Δ::At_cad-Pk_mttA* strain from the YPD agar plate to a 250-mL flask containing 50-mL YPD medium. The seed cells were grown in the flask for 24 h at 30 °C, 250 rpm until an OD_{600} of 2–2.5 was reached. The entire 50-mL culture was then transferred to a 1-L fermenter (Biostat B-DCU, Sartorius, Germany) to initiate the fed-batch fermentation (t = 0 h). The initial volume of the fermentation medium was 0.6 L, containing Fisher yeast extract (20.0 g/L), Bacto™ peptone (10.0 g/L), glucose (20.0 g/L), and antifoam 24, at 1.0 mL/L). The dissolved oxygen level (measured by pO_2) was set at 25% of air saturation by cascade controls of the agitation speed between 150 and 650 rpm. The aeration rate was fixed at 0.3 L/min in general or specified otherwise. The temperature was maintained at 30 °C throughout the run. The initial pH value was measured as 6.1, and no acid or base was used to control the pH during the process. Glucose feeding was started (using a 600 g/L stock solution) when the concentration in the medium decreased below 5 g/L. The glucose concentration was brought back to about 20 g/L and maintained at this level during the remainder of the run by adjusting the glucose feed rate based on an off-line glucose measurement. The fed-batch fermentation was performed with two biological replicates.

2.8. HPLC analysis

After centrifugation at 12,000 rpm for 5 min, the cell-free medium was filtered through a 0.2-μm syringe filter (XPERTEK, St. Louis, MO) before HPLC analysis. A Waters HPLC system (Waters, Milford, MA) was used, consisting of a binary HPLC pump, a 717 plus auto sampler, a column heater module, a 2998 photodiode array detector, and an Aminex HPX-87H column (300 × 7.8 mm) (Bio-Rad, Hercules, CA). The following program was applied: 0.3 mL/min; 30 °C; mobile phase, 5 mM sulfuric acid; loading volume, 10 μL; running time, 60 min/sample. The signals at 210 nm were extracted and compared to the standard curves of the authentic IA purchased from Sigma-Aldrich (St. Louis, MO).

2.9. Fluorescence microscopy imaging

Yeast strains were cultivated in YPD medium supplemented with 10 g/L IA for 10 h (starting OD_{600} = 0.2). The cells were subsequently concentrated approximately 20-fold by centrifugation and incubated with 5 μM SYTO 9 green fluorescent nucleic acid stain and 55 μM propidium iodide red fluorescent nuclear counterstain (LIVE/DEAD BacLight Viability Kit L-7007, Life Technologies) for 35 min. The "dead" reference samples were prepared by mixing 200 μL of cells with 200 μL of 20% isopropyl alcohol for 3 min prior to staining.

Specimens were prepared by placing a small droplet of cells stained with the fluorescence dye mixture on clean glass coverslips (thickness 1, 22 mm × 22 mm). The yeast cells were imaged with a Zeiss Axioplan II microscope equipped with AxioCam color and B/W digital cameras operating in bright field, phase-contrast, polarizing, dark-field, fluorescence, and Nomarski (DIC) optical modes. Green fluorescence (EGFP filter - excitation: 470/40 band pass; emission: 525/50 band pass), red fluorescence (Rhodamine 20 filter - excitation: 546/12 band pass; emission: 607/80 band pass), and transmission bright field images of the cells (deposited on the glass coverslips and placed upside down on regular microscope glass slides) were acquired with a 40× objective lens and monochrome camera. The images were acquired and analyzed using Zeiss Zen Black and Zeiss Zen Lite software.

3. Results

3.1. Initial development of the host strain and the expression vector

Five *P. kudriavzevii* strains requested from the ARS Culture Collection (NRRL) were evaluated for their IA tolerance and compared with two commonly used *S. cerevisiae* laboratory strains (one haploid and one diploid) that served as references. In one set of conditions, the testing concentrations of IA varied in a range of 0–50 g/L without pH adjustment, while in the other set, the initial pH values of the media supplemented with IA at different concentrations were consistently adjusted to 5.6. The cells were inoculated with an initial OD_{600} of 0.2 and the growths were measured after cultivation for 10 h. When the pH was not adjusted, the *S. cerevisiae* strains barely grew in the presence of 10 g/L IA, whereas the impact on the growths of the five *P. kudriavzevii* strains was small (Fig. 1a). Among these, the OD_{600} of the best performer (YB4010) decreased by only 10% at 10 g/L (and 63% at 20 g/L). With pH adjustment, at 50 g/L of IA, the OD_{600} values of the *S. cerevisiae* strains were 24% to 56% of those without IA supplementation (Fig. 1b); very little detrimental impact was observed for *P. kudriavzevii* even at high concentrations, and all five strains could grow to higher OD_{600} with IA supplementation. These results support the use of *P. kudriavzevii* as a better-suited IA production host than *S. cerevisiae*. A version of the top performer, *P. kudriavzevii* YB4010, was subsequently made auxotrophic for uracil by transforming a 1-kb fragment carrying the 500-bp homologous arms to the upstream and the downstream regions of the *URA3* locus. This *P. kudriavzevii ura3Δ* strain was used for all the subsequent studies.

An episomal plasmid, pWS-Pk-URA-GFP (Fig. S1), was constructed using the previously reported DNA assembler method (Shao et al., 2012; Shao and Zhao, 2014). This shuttle plasmid carries the *URA3* selection marker cloned from the genome of *P. kudriavzevii*, a previously identified 91-bp autonomously replicating sequence (*ARS*) (Xiao et al., 2014), and a *GFP* expression cassette that is used to monitor plasmid stability; it also includes the genetic elements to facilitate plasmid assembly in *S. cerevisiae via* homologous recombination and plasmid enrichment in *E. coli*. As a typical phenomenon observed for yeast strains, if the plasmid does not carry the centromeric sequence required for directing stable DNA segregation during cell division, a broader GFP^+ expression peak will be observed, indicating that there is an variation in the plasmid copy number among the progeny cells (Fig. S2). In a single culture, 64% of the *P. kudriavzevii* cells transformed with the plasmid pWS-Pk-URA-GFP expressed GFP after cultivation for 24 h. As a reference, this percentage for using a commercial *S. cerevisiae* vector was 80%, but the variation of GFP expression among the *S. cerevisiae* cells was much smaller. The plasmid backbone of pWS-Pk-URA-GFP carrying the *URA3* selection marker and the *ARS* sequence was used for screening the beneficial combinations of the gene manipulations at the initial stage.

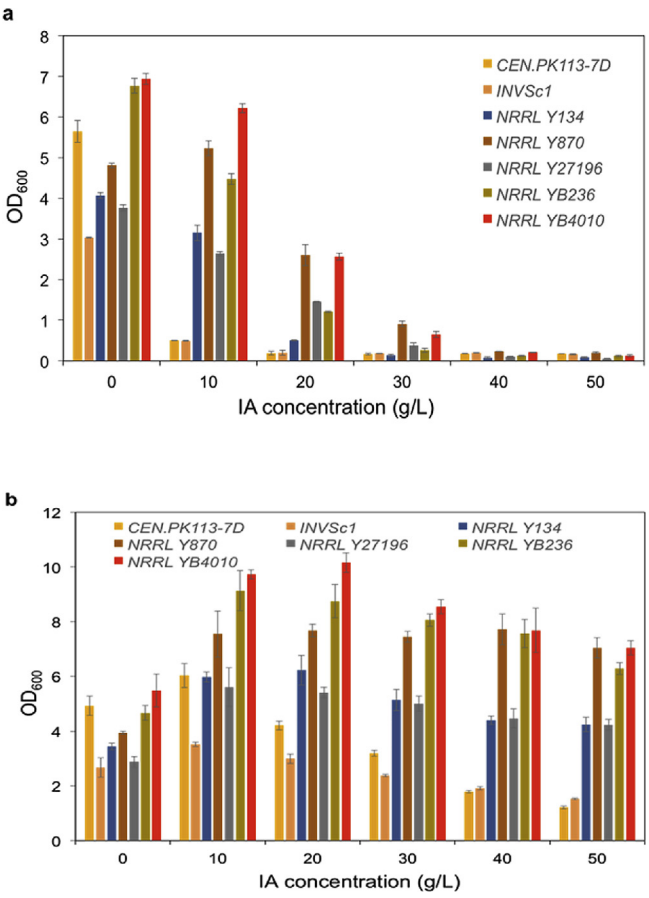

Fig. 1. Cell growth in the SC medium containing different concentrations of IA. **a**. no pH adjustment; **b**. the initial pH values adjusted to 5.6.

3.2. Heterologous production of IA in P. kudriavzevii

As *S. cerevisiae* and *P. kudriavzevii* have a similar codon usage preference, *At_cad* was codon-optimized according to the codon preference in *S. cerevisiae* and cloned into the aforementioned plasmid backbone (named pWS-URA-Cad, Fig. S1) (Fig. 2). The resulting transformed strain was able to produce IA at 135 ± 5 mg/L after a five-day cultivation period in SC-URA medium (Fig. 3).

Previous studies in *A. terreus* identified one transporter (encoded by *mttA*) in the IA biosynthetic gene cluster (van der Straat et al., 2014). At_MttA is a mitochondrial tricarboxylate transporter believed to promote the transport of *cis*-aconitate from mitrochondria to cytosol (Steiger et al., 2013) (Fig. 2). Using At_mttA as a query, we found a putative transporter in *P. kudriavzevii via* BLAST. The protein C5L36_0C10570 shares an identity of 38.38% with At_MttA (hereafter named Pk_MttA). We overexpressed the candidate transporter together with the codon-optimized At_Cad. The results supported that Pk_MttA enhanced the transport of *cis*-aconitate to the cytosol, where *cis*-aconitate was further converted to 245 ± 11.3 mg/L IA by At_Cad (Fig. 3).This result suggests that the availability of *cis*-aconitate is the limiting step for IA production in *P. kudriavzevii*, a phenomenon that has also been observed in other systems including in *A. niger* (Blumhoff et al., 2013; Steiger et al., 2016; van der Straat et al., 2014) and *U. maydis* (Geiser et al., 2016).

3.3. Development of CRISPR-editing tool and genome integration of the IA pathway

As *P. kudriavzevii* is a relatively new host with limited genetic manipulation tools, we decided to develop a CRISPR-Cas9 editing system for this strain. This aim was also motivated by the fact that *P. kudriavzevii* is a diploid species, so the traditional gene deletion strategy involves a laborious sequential procedure requiring first deletion of one copy of the target gene, followed by the recycling of the selection marker, and finally knocking out of the second copy. To properly transcribe the synthetic guide RNA (sgRNA), we adopted the promoter of *RPR1* (encoding the RNA component of RNase P), which can be recognized by RNA polymerase III. The gene *ADE2* was chosen as the first target because its disruption renders an easily screenable pink appearance to the transformants. Real-time PCR was conducted to verify that the sgRNA designed to target *ADE2* was successfully transcribed (Fig. S3a). Next, five versions of *Cas9* genes together with RPR1p-sgRNA^{ade2} were individually cloned into the aforementioned *P. kudriavzevii* plasmid backbone and their activities to knockout *ADE2* gene were evaluated. These versions included the original sequence of the *Cas9* gene from *Streptococcus pyogenes* (Sp_Cas9) (Cong et al., 2013), Sp_Cas9 with two mutations D147Y and P411T (named Sp_iCas9; supposed to have a higher activity than Cas9) (Bao et al., 2015), the codon-optimized sequences implemented in two other yeast species, *Candida albicans* (Ca_Cas9) (Vyas et al., 2015) and *Scheffersomyces stipites* (Ss_Cas9)(Cao et al., 2018), and the codon-optimized version used in *Homo sapiens* (Hs_Cas9) (DiCarlo et al., 2013). Among them, Sp_iCas9 demonstrated the highest disruption efficiency of 42% (Figs. S3b and S3c), whereas the other four versions had disruption efficiencies ranging from 8% to 28%. Sequencing the *ade2* locus confirmed that an *indel* mutation has occurred (Fig. S3d). Based on these results, Sp_iCas9 and the RPR1 promoter were selected for the subsequent genome-editing endeavors.

Considering the instability of the plasmid and the resulting inhomogenous expression in *P. kudriavzevii* (Fig. S2), we decided to integrate both *At_Cad* and *Pk_MttA* to the genome using CRISPR. A plasmid bearing the CRISPR elements targeting *ADE2* and a donor DNA carrying the *URA3*, *At_Cad*, and *Pk_MttA* expression cassettes flanked by the 500-bp upstream and downstream sequences of *ADE2* were constructed (Fig. S1) and transformed into the *P. kudriavzevii Δura3* strain. The integration of *At_Cad* and *Pk_MttA* was confirmed by PCR and sequencing (Fig. S4). Fermentation conducted in the same SC-URA medium showed that the genome integration improved the production of IA to 401 ± 12.4 mg/L (Fig. 3).

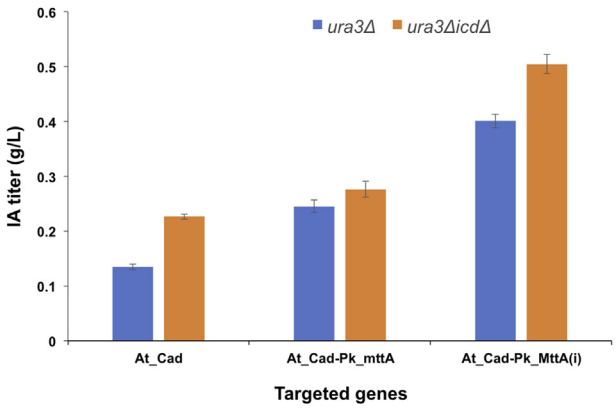

Fig. 3. IA production after 5-day fermentation in shaking flasks with genetic manipulations. At_Cad, *cis*-aconitate decarboxylase (cloned from *A. terreus*); Pk_MttA, mitochondrial tricarboxylate transporter; At_Cad-Pk_MttA (i), integration of the expression cassettes of *URA3*, *At_cad*, and *Pk_mttA* into the genome; ICD, isocitrate dehydrogenase.

3.4. Deletion of isocitrate dehydrogenase

Another potential strategy to enhance the production of IA in *P. kudriavzevii* is to delete the downstream competing pathway in order to increase the availability of the precursor *cis*-aconitate. Isocitrate dehydrogenase (ICD) catalyzes the oxidative decarboxylation of isocitrate for α-ketoglutarate synthesis (Fig. 2). The sgRNA was designed based on the CHOPCHOP web tool (Montague et al., 2014) for targeting the two copies of the *ICD* gene. The double-stranded DNA breaks were repaired using the co-transformed donor DNA carrying the 500 bp upstream and downstream homologous sequences of the open reading frame of *ICD*. Seven colonies were inoculated, and the subsequent PCR verification (Fig. S4), together with sequencing analysis, confirmed that all of them carried the expected deletion of both copies of *ICD*, indicating the high competency of the CRISPR tool in editing the genome of a diploid strain (Fig. S4b).

The aforementioned plasmids were then transformed into the *ura3ΔicdΔ* strain; meanwhile, the *At-Cad-Pk_MttA* expression cassettes were re-integrated into this deletion strain. All of the strains with an *ICD* deletion demonstrated higher IA production levels than their counterparts in the *ura3Δ* strain (Fig. 3), among which, the strain with the integrated *At-Cad-Pk_MttA* reached the highest titer of 505 ± 17.7 mg/L,

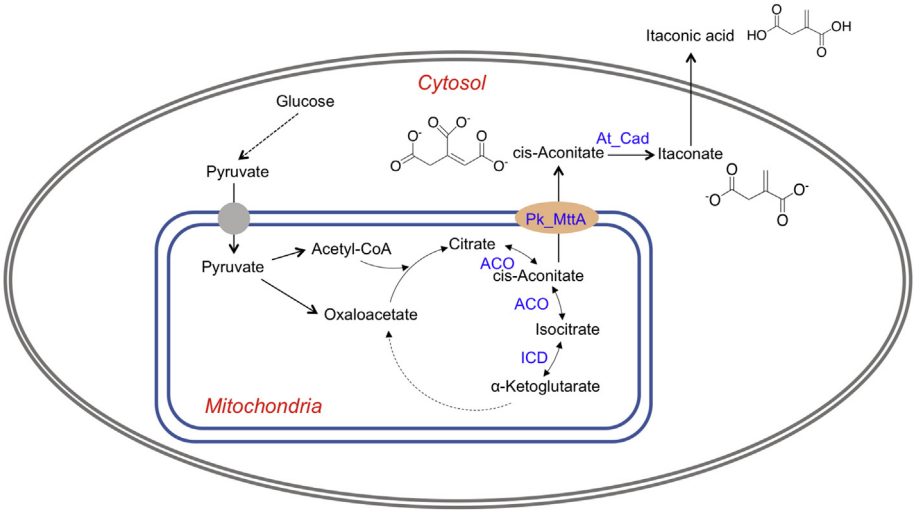

Fig. 2. Metabolic pathway for itaconic acid production in *P. kudriavzevii*.ACO, acotinase; ICD: isocitrate dehydrogenase; At_Cad, *cis*-aconitate decarboxylase (cloned from *A. terreus*); Pk_MttA, mitochondrial tricarboxylate transporter. Note that the the transporter was specified with the name of the host to be differentiated with the one sourced from *A. terreus*.

which is 3.7-fold of the level obtained by the starting strain, with *At-Cad* being overexpressed by the plasmid.

Having the IA pathway in the integrated form granted us the flexibility of using non-selective medium. Fed-batch fermentation was conducted for the *P. kudriavzevii ura3Δicd1Δade2Δ::At_cad-Pk_mttA* strain in the YPD medium for 96 h using a 1-L fermenter. The production of IA climbed to 1232 ± 64 mg/L at 24 h with a yield of 29 ± 1.2 mg IA/g glucose and a productivity of 51 mg/L/h (Fig. 4). The titer was increased slightly and stably maintained until the end of fermentation. Without any human interference, the pH of the cultures dropped significantly from 6.1 to 4.7 in the first 6 h, then further decreased to, and remained at about 3.9 throughout the rest of the process.

4. Discussion

In the past decade, several IA heterologous producers using homogenous cultures have been developed in laboratory (Table 1). Due to low acid tolerance, the cultivation of bacterial hosts (e.g., *E. coli* and *C. glutamicum*) is usually carried out at pH higher than 5. A simple calculation based on the dissociation constants of IA (pK_{a1} = 3.85 and pK_{a2} = 5.55) showed that at pH 5.6 (the condition used in the IA tolerance assay), the percentage of the desired undissociated form of IA is less than 1%. In order to maintain the majority of the produced IA in the undissociated form (e.g., >97%), the pH needs to be reduced to a level below 2.3, which is not suitable for cultivating most microbial hosts. The advantage of developing an acid-tolerant production host appeared more obvious in the industrial-scale processes due to the cost and effort saved in the excessive downstream processing and the reduced impact on the environment. Little is known on how IA of stressful concentrations affects the physiology of fungal cells but the previous studies that used *S. cerevisiae* as a surrogate to study the fungal responses to organic acids clearly demonstrated that the internal accumulation of organic acids resulted in multiple deleterious effects such as damaging of the plasma membrane structure (Mira et al., 2010). Compared to *S. cerevisiae*, *P. kudriavzevii* demonstrates much higher tolerance of IA in the medium with unadjusted pH (Fig. 1). In order to further check whether *P. kudriavzevii* maintains its membrane integrity more effectively than *S. cerevisiae*, we cultivated both strains in the medium with 10 g/L IA supplementation for 10 h, and assessed their membrane integrity by a fluorescence microscope. The membrane-permeable dye SYTO9 displays a green fluorescence when bound to DNA; the other dye propidium iodide is membrane-impermeable, and only fluoresces red in the cells with damaged membranes. As shown in Fig. 5, *S. cerevisiae* demonstrated much more compromised membranes than *P. kudriavzevii* when the pH was not controlled.

Studies have shown that to avoid this acid-induced toxic effect, *S. cerevisiae* relies on exporters to reduce the internal concentration of the acid anion and also reinforces cell envelope to avoid the re-entry of the undissociated acid (Mira et al., 2010). Whether *P. kudriavzevii* is more tolerant to IA because it is more impermeable to its entry (e.g., due to the structure of the cell wall or of the plasma membrane that reduces diffusion of undissociated IA molecules) or if it has more efficient IA export mechanisms (or both) remain intriguing to explore in the future. The fact that higher tolerance of *P. kudriavzevii* is observed not only for IA but also for other organic acids as well (Park et al., 2018; Toivari et al., 2013; Xiao et al., 2014) suggests that at least the first hypothesis plays an important role.

A comparison should also be made with *Y. lipolytica*, a host characterized to be resistant to IA in a recent study (Zhao et al., 2019). The initial titer achieved by overexpressing *At_Cad* in the *Y. lipolytica* po1f strain was 0.363 g/L, which was improved by the heterologous expression of *A. terreus* mitochondrial tricarboxylate transporter (At_MttA) by an impressive 10.6-fold. In *A. niger*, overexpression of At_MttA also showed a 24.8-fold increase (van der Straat et al., 2014). Different from these works, in our study we have identified an endogenous *P. kudriavzevii* transporter that can serves as a *cis*-acconitate transporter.

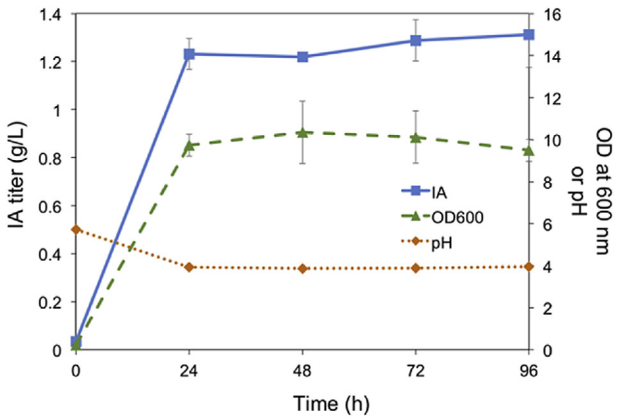

Fig. 4. Production of IA in fed-batch fermentation mode.

This is, to the best of our knowledge, the first description of such a transporter identified from a host other than the native IA producers. This endogenous transporter shares an identity of 38.38% and 40.94% with At_MttA and Um_Mtt1 (the *U. maydis* mitochondrial tricarboxylate transporter), respectively, and a higher identity of 63.45% with the *S. cerevisiae* mitochondrial citrate transport protein Sc_Ctp1. The overexpression or heterologous expression of Um_Mtt1 and At_MttA has been extensively recognized as a strategy to improve the production of IA by increasing the *cis*-aconitate pool in the cytosol (Wierckx et al., 2020). Besides citrate and *cis*-aconitate, all three transporters were shown to be able to transport other TCA cycle intermediates with different levels of activity (Xu et al., 2000; Scarcia et al., 2019), and their localization on the mitochondrial membranes have been confirmed (Palmieri et al., 1972; Steiger et al., 2016; Geiser et al., 2016). Previous study has also shown that there are two citrate-binding sites in Sc_Ctp1 that include nine crucial amino acids (K37, K83, R87, G119, R181, R189, K239, R276 and R279) (Aluvila et al., 2010). All these nine amino acids are conserved in *Pk_MttA* as well as At_MttA and Um_Mtt1 (Fig. S5). Based on all these information, it is possible that *Pk_MttA* is a mitochondrial citrate transport protein which is also able to transport *cis*-aconitate. The substrate specificity of *Pk_MttA* towards various TCA cycle intermediates can be performed in the future by methods such as transport assay using purified transporters and reconstituted liposomes (Scarcia et al., 2019). The fact that the improvements registered in other systems upon the use of At_MttA are higher than the one observed in our work suggests that *A. terreus*, as the native IA producer, might have evolved a transport system more specific to the IA biosynthesis, especially considering that the genes encoding *Cad* and *MttA* co-localize in the same gene cluster in *A. terreus*. Its applicability in *P. kudriavzevii* will be evaluated in our future work, which will also entail the comparison with a multi-copy integrated version of *Pk_MttA*. Nonetheless, the demonstration of at least one novel *cis*-aconitate transporter opens the possibility of additional manipulations to eventually explore other yet uncharacterized transporters that may present improved activities than At_MttA.

In the fed-batch fermentation, we also noticed that cell density stopped increasing after 9 h. However, the residual glucose concentrations in the medium were still in the range of 7–34 g/L for the period of 12 h to 96 h, suggesting that bottlenecks other than the amount of carbon source constrained the productivity. This result was not fully expected because IA should not exert an obvious inhibitory impact on growth at the current titer. In the IA tolerance assay conducted in the shaking flasks, even in the presence of 10 g/L IA, the OD_{600} measured at 10 h cultivation was 90% of that without IA supplementation (Fig. 1a). One potential explanation is the discrepancy between intracellular production of IA in the fermentation versus the extracellular IA tolerance assay. In the engineered strain under fermentation conditions, the buildup of the produced IA in the mitochondria and/or the cytosol and the resultant high local concentrations may result in a more harmful impact compared

Table 1
Production of IA by heterologous microbial hosts with homogenous cultures.

Hosts	Titer (g/L)	Yield (g/g)	Productivity (g/L/h)	pH	Fermentation type	Reference
No pH adjustment during the fermentation						
Pichia kudriavzevii	1.232	0.029	0.0513	Final pH dropped to 3.9	Fed-batch	This study
Yarrowia lipolytica	22.03	0.056	0.111	Final pH dropped to 2.38	Fed-batch	Zhao et al. (2019)
Saccharomyces cerevisiae	0.815	0.041	0.00485	Starting at 5.0	Batch	Young et al. (2018)
pH was adjusted to more favorable condition						
Escherichia coli	47	0.448	0.39	6.9	Fed-batch	Harder et al. (2018)
Corynebacterium glutamicum	7.8	0.29	0.27	7.0	Batch	Otten et al. (2015)

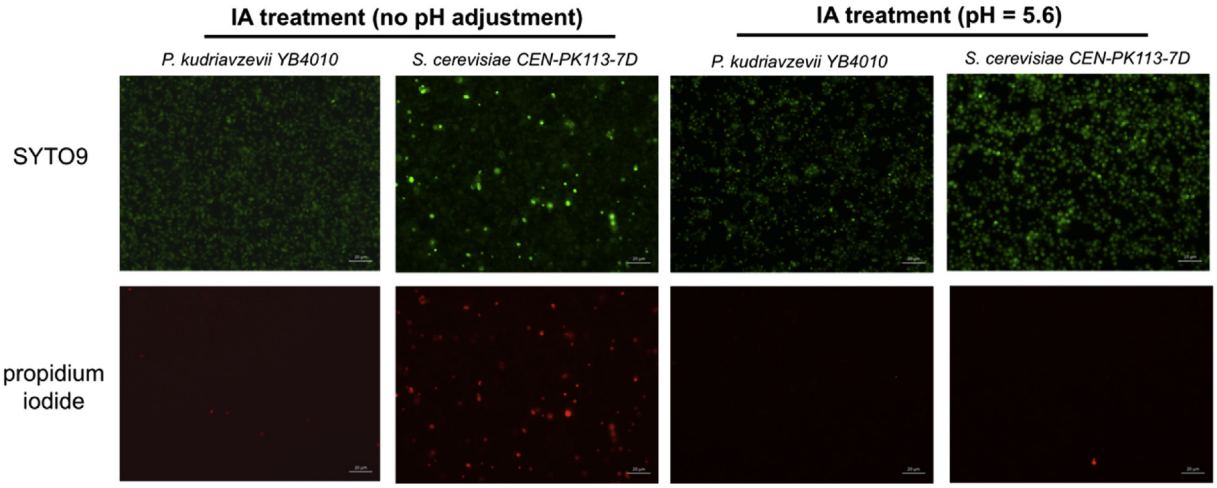

Fig. 5. Membrane integrative analysis with a fluorescence microscope. *S. cerevisiae* and *P. kudriavzevii* were cultivated in the medium with 10 g/L IA supplementation for 10 h. Cells with undamaged membranes only fluoresced green, whereas cells with compromised membranes fluoresced both green and red, indicating that propidium iodide entered the nucleus and bound to the nucleic acids. (For interpretation of the references to color in this figure legend, the reader is referred to the Web version of this article.)

to the extracellular IA supplemented to the medium, reiterating the need to quickly export IA to the medium. Alternative solutions for future optimization relevant to the fermentation process might include (1) using inducible promoters to ensure that the IA pathway is turned on after a high cell density is achieved, or (2) applying a glucose-limiting condition during the initial cell growth stage to constrain the usage of glucose for growth, followed by a continuous feeding mode to accelerate production.

5. Conclusions

Considering the multiple practical aspects involved in large-scale industrial fermentation processes, the development of acid-tolerant hosts for organic acid production is essential. Joining the previous works for the production of xylonic acid, lactic acid, and succinic acid (Park et al., 2018; Toivari et al., 2013; Xiao et al., 2014) this study demonstrates the potential use of *P. kudriavzevii* as a generic production platform for many organic acids and provides effective genetic manipulation tools that have not been offered by the previous engineering efforts in this species. The bottlenecks identified in this study pave the way for future endeavors to improve the production of IA, eventually to a commercially attractive level.

Declarations of competing interest

The authors declare no competing financial interests.

CRediT authorship contribution statement

Wan Sun: Conceptualization, Methodology, Investigation, Writing - original draft. **Ana Vila-Santa:** Investigation. **Na Liu:** Investigation. **Tanya Prozorov:** Investigation. **Dongming Xie:** Investigation. **Nuno Torres Faria:** Investigation. **Frederico Castelo Ferreira:** Investigation. **Nuno Pereira Mira:** Conceptualization, Supervision, Writing - review & editing. **Zengyi Shao:** Conceptualization, Methodology, Supervision, Writing - original draft, Writing - review & editing, Funding acquisition, Project administration.

Acknowledgments

This work was supported by the National Science Foundation Grant (MCB 1716837) and the U.S. Department of Energy, Office of Science, Biological and Environmental Research through Ames Laboratory. Ames Laboratory is operated for the U.S. Department of Energy by Iowa State University under Contract No. DE-AC02-07CH11358.

Research undertaken at the Institute for Bioengineering and Biosciences (iBB) at Instituto Superior Técnico was supported by Fundação para a Ciência e a Tecnologia (through contracts UID/BIO/04565/2019 and ERA-IB-2-6/0003/2014 and a PhD grant to AVS-PD/BD/114151/2015). The research was also supported by the EraNet in Industrial Biotechnology (6th edition) through the TTRAFFIC (Toxicity and Transport for Fungal production of Industrial Compounds) project. Support received from Programa Operacional Regional de Lisboa 2020 (project no. 007317) is also acknowledged.

The authors would like to acknowledge the assistance provided by the Roy J. Carter High Resolution Microscopy Facility with fluorescence microscopy imaging conducted in this study, as well as the support given by Master students at iBB, André Costa and Joana Vicente.

Appendix A. Supplementary data

Supplementary data to this article can be found online at https://doi.org/10.1016/j.mec.2020.e00124.

References

Aluvila, S., Kotaria, R., Sun, J., Mayor, J.A., Walters, D.E., Harrison, D.H., Kaplan, R.S., 2010. 'The yeast mitochondrial citrate transport protein molecular determinants of its substrate specificity. J. Biol. Chem. 285 (35), 27314–27326.

Bao, Z., Xiao, H., Liang, J., Zhang, L., Xiong, X., Sun, N., Si, T., Zhao, H., 2015. 'Homology-integrated CRISPR-Cas (HI-CRISPR) system for one-step multigene disruption in *Saccharomyces cerevisiae*. ACS Synth. Biol. 4, 585–594.

Blazeck, J., Hill, A., Jamoussi, M., Pan, A., Miller, J., Alper, H.S., 2015. 'Metabolic engineering of *Yarrowia lipolytica* for itaconic acid production. Metab. Eng. 32, 66–73.

Blazeck, J., Miller, J., Pan, A., Gengler, J., Holden, C., Jamoussi, M., Alper, H.S., 2014. 'Metabolic engineering of *Saccharomyces cerevisiae* for itaconic acid production. Appl. Microbiol. Biotechnol. 98, 8155–8164.

Blumhoff, M.L., Steiger, M.G., Mattanovich, D., Sauer, M., 2013. 'Targeting enzymes to the right compartment: metabolic engineering for itaconic acid production by *Aspergillus niger*. Metab. Eng. 19, 26–32.

Cao, M., Gao, M., Ploessl, D., Song, C., Shao, Z., 2018. 'CRISPR-mediated genome editing and gene repression in *Scheffersomyces stipitis*. Biotechnol. J. 13, e1700598.

Choi, S., Song, C.W., Shin, J.H., Lee, S.Y., 2015. 'Biorefineries for the production of top building block chemicals and their derivatives. Metab. Eng. 28, 223–239.

Cong, L., Ran, F.A., Cox, D., Lin, S., Barretto, R., Habib, N., Hsu, P.D., Wu, X., Jiang, W., Marraffini, L.A., Zhang, F., 2013. Multiplex genome engineering using CRISPR/Cas systems. Science 339, 819–823.

Curran, K.A., Alper, H.S., 2012. Expanding the chemical palate of cells by combining systems biology and metabolic engineering. Metab. Eng. 14, 289–297.

De Carvalho, J.C., Magalhaes, A.I., Soccol, C.R., 2018. 'Biobased itaconic acid market and research trends—is it really a promising chemical. Chim. Oggi-Chem. Today 36, 56–58.

De Hoog, G.S., 1996. 'Risk assessment of fungi reported from humans and animals. Mycoses 39, 407–417.

DiCarlo, J.E., Norville, J.E., Mali, P., Rios, X., Aach, J., Church, G.M., 2013. Genome engineering in *Saccharomyces cerevisiae* using CRISPR-Cas systems. Nucleic Acids Res. 41, 4336–4343.

El-Imam, A.A., Du, C., 2014. 'Fermentative itaconic acid production. J Biodivers Biopros Dev 1, 1–8.

Geiser, E., Przybilla, S.K., Friedrich, A., Buckel, W., Wierckx, N., Blank, L.M., Bölker, M., 2016. '*Ustilago maydis* produces itaconic acid via the unusual intermediate trans-aconitate. Microb Biotechnol 9, 116–126.

Harder, B.J., Bettenbrock, K., Klamt, S., 2016. 'Model-based metabolic engineering enables high yield itaconic acid production by *Escherichia coli*. Metab. Eng. 38, 29–37.

Harder, B.J., Bettenbrock, K., Klamt, S., 2018. 'Temperature-dependent dynamic control of the TCA cycle increases volumetric productivity of itaconic acid production by *Escherichia coli*. Biotechnol. Bioeng. 115, 156–164.

Hossain, A.H., Li, A., Brickwedde, A., Wilms, L., Caspers, M., Overkamp, K., Punt, P.J., 2016. 'Rewiring a secondary metabolite pathway towards itaconic acid production in *Aspergillus niger*. Microb. Cell Factories 15, 130.

Krull, S., Hevekerl, A., Kuenz, A., Prüße, U., 2017. 'Process development of itaconic acid production by a natural wild type strain of *Aspergillus terreus* to reach industrially relevant final titers. Appl. Microbiol. Biotechnol. 101, 4063–4072.

Mira, N.P., Teixeira, M.C., Sá-Correia, I., 2010. 'Adaptive response and tolerance to weak acids in *Saccharomyces cerevisiae*: a genome-wide view. Omics 14, 525–540.

Montague, T.G., Cruz, J.M., Gagnon, J.A., Church, G.M., Valen, E., 2014. 'CHOPCHOP: a CRISPR/Cas9 and TALEN web tool for genome editing. Nucleic Acids Res. 42, W401–W407.

Otten, A., Brocker, M., Bott, M., 2015. 'Metabolic engineering of *Corynebacterium glutamicum* for the production of itaconate. Metab. Eng. 30, 156–165.

Palmieri, F., Stipani, L., Quagliariello, E., Klingenberg, M., 1972. 'Kinetic study of the tricarboxylate carrier in rat liver mitochondria. Eur. J. Biochem. 26, 587–594.

Park, H.J., Bae, J.H., Ko, H.J., Lee, S.H., Sung, B.H., Han, J.I., Sohn, J.H., 2018. 'Low-pH production of d-lactic acid using newly isolated acid tolerant yeast *Pichia kudriavzevii* NG7. Biotechnol. Bioeng. 115, 2232–2242.

Porro, D., Branduardi, P., 2017. 'Production of Organic Acids by Yeasts and Filamentous fungi.' Biotechnol of Yeasts and Filamentous Fungi. Springer.

Saha, B.C., 2017. 'Emerging biotechnologies for production of itaconic acid and its applications as a platform chemical. J. Ind. Microbiol. Biotechnol. 44, 303–315.

Shao, Z., Luo, Y., Zhao, H., 2012. 'DNA assembler method for construction of zeaxanthin-producing strains of *Saccharomyces cerevisiae*. Methods Mol. Biol. 898, 251–262.

Shao, Z., Zhao, H., 2014. 'Manipulating natural product biosynthetic pathways via DNA assembler. Curr Protoc Chem Biol 6, 65–100. Steiger, Matthias G, Peter J Punt, Arthur.

Scarcia, P., Gorgoglione, R., Messina, E., Fiermonte, G., Blank, L.M., Wierckx, N., Palmieri, L., Agrimi, G., 2019. Mitochondrial carriers of *Ustilago maydis* and *Aspergillus terreus* involved in itaconate production: same physiological role but different biochemical features. FEBS (Fed. Eur. Biochem. Soc.) Lett. https://doi.org/10.1002/1873-3468.13645.

Steiger, M.G., Punt, P.J., Ram, A.F., Mattanovich, D., Sauer, M., 2016. Characterizing MttA as a mitochondrial cis-aconitic acid transporter by metabolic engineering. Metab. Eng. 35, 95–104.

Steiger, M.G., Blumhoff, M.L., Mattanovich, D., Sauer, M., 2013. 'Biochemistry of microbial itaconic acid production. Front. Microbiol. 4, 23.

Tehrani, H.H., Tharmasothirajan, A., Track, E., Blank, L.M., Wierckx, N., 2019. 'Engineering the morphology and metabolism of pH tolerant *Ustilago cynodontis* for efficient itaconic acid production. Metab. Eng. 54, 293–300.

Toivari, M., Vehkomäki, M.L., Nygård, Y., Penttilä, M., Ruohonen, L., Wiebe, M.G., 2013. 'Low pH D-xylonate production with *Pichia kudriavzevii*. Bioresour. Technol. 133, 555–562.

Tran, K.N.T., Somasundaram, S., Eom, G.T., Hong, S.H., 2019. 'Efficient itaconic acid production via protein-protein scaffold introduction between GltA, AcnA, and CadA in recombinant *Escherichia coli*. Biotechnol. Prog. 3, e2799.

van der Straat, L., Vernooij, M., Lammers, M., van den Berg, W., Schonewille, T., Cordewener, J., van der Meer, I., Koops, A., de Graaff, L.H., 2014. 'Expression of the Aspergillus terreus itaconic acid biosynthesis cluster in *Aspergillus niger*. Microb. Cell Factories 13, 11.

Vuoristo, K.S., Mars, A.E., Sangra, J.V., Springer, J., Eggink, G., Sanders, J.P., Weusthuis, R.A., 2015. 'Metabolic engineering of the mixed-acid fermentation pathway of *Escherichia coli* for anaerobic production of glutamate and itaconate. Amb. Express 5, 61.

Vyas, V.K., Barrasa, M.I., Fink, G.R., 2015. 'A *Candida albicans* CRISPR system permits genetic engineering of essential genes and gene families. Sci Adv 1, e1500248.

Werpy, T., Petersen, G., 2004. Top Value Added Chemicals from Biomass: Volume I-Results of Screening for Potential Candidates from Sugars and Synthesis Gas. National Renewable Energy Lab., Golden, CO (US).

Wierckx, N., Agrimi, G., Lübeck, P.S., Steiger, M.G., Mira, N.P., Punt, P.J., 2020. 'Metabolic specialization in itaconic acid production: a tale of two fungi. Curr. Opin. Biotechnol. 62, 153–159.

Xiao, H., Shao, Z., Jiang, Y., Dole, S., Zhao, H., 2014. Exploiting *Issatchenkia orientalis* SD108 for succinic acid production. Microb. Cell Factories 13, 121.

Xu, Y., Kakhniashvili, D.A., Gremse, D.A., Wood, D.O., Mayor, J.A., Walters, D.E., Kaplan, R.S., 2000. 'The yeast mitochondrial citrate transport protein. Probing the roles of cysteines, Arg(181), and Arg(189) in transporter function. J. Biol. Chem. 275 (10), 7117–7124.

Young, E.M., Zhao, Z., Gielesen, B.E., Wu, L., Gordon, D.B., Roubos, J.A., Voigt, C.A., 2018. 'Iterative algorithm-guided design of massive strain libraries, applied to itaconic acid production in yeast. Metab. Eng. 48, 33–43.

Zhao, C., Cui, Z., Zhao, X., Zhang, J., Zhang, L., Tian, Y., Qi, Q., Liu, J., 2019. 'Enhanced itaconic acid production in *Yarrowia lipolytica* via heterologous expression of a mitochondrial transporter MTT. Appl. Microbiol. Biotechnol. 103, 2181–2192.